IEEE Access
Multidisciplinary | Rapid Review | Open Access Journal

Received November 3, 2021, accepted November 15, 2021, date of publication November 17, 2021,
date of current version November 29, 2021.

Digital Object Identifier 10.1109/ACCESS.2021.3128910

Research on Clearance Elimination Control Based on Linearization

TONG FENG, JIANAN SUN, JINJI QIU, AND SHUANGHUI HAO
School of Mechatronics Engineering, Harbin Institute of Technology, Harbin 150001, China
Corresponding author: Shuanghui Hao (156490479@qq.com)

ABSTRACT The accuracy and operational stability of a turntable system can be reduced by the backlash problem that occurs in the reducer's gear transmission system. To solve this problem, this work proposes a scheme in which two motors are used to eliminate the effects of backlash through a linearization process. By calculating and outputting two independent torques synchronously from the two servo motors to the system output shaft's gears, a nonlinear system with backlash can be transformed into a linear system without backlash, thus making the resulting system easy to control. Experiments verify that the system will remain stable after the movement of the output shaft stops.

INDEX TERMS Backlash, double-motor system, gear transmission system, linearization algorithm.

I. INTRODUCTION

Turntable systems are currently used in a wide range of industrial applications, from machine tools to robotics and aviation. To ensure that the turntable will run stably and accurately in these systems, a servo motor is often used to drive the turntable. Servo motors generally offer high rotation speeds and output relatively low torques, but turntable systems conversely require low rotation speeds and high output torques, and gear transmission systems are thus used as reducers in servo turntable systems.

In the gear transmission system, backlash from the gear clearance can cause system shock and hysteresis errors. Through construction and analysis of gear models, several studies [1]–[3] have proved that different effects could be caused by backlash, including meshing force impact, torque instability, cumulative damage to the gear system, and reduced transmission accuracy.

Mechanical methods and electrical methods offer two different ways to reduce the effects of backlash. Mechanical methods mainly focus on the structures of the gears and the transmission systems. Reference [4] analyzed the meshing characteristics of both anti-backlash single-roller and anti-backlash double-roller enveloping hourglass worm gears. The rotary vector (RV) reducer provides low transmission backlash but has a complex structure, and [5] therefore proposed a matching algorithm and applied it to selective assembly of the RV reducer to realize high assembly accuracy. Reference [6] proposed a new tooth profile modification method for cycloidal gears that can be used in precision reducers or RV reducers. This method produced better meshing characteristics and improved transmission performance. Reference [7] designed a new type of cylindrical gear with tapered teeth and used it in a reducer. This gear enabled adjustment of the backlash between the flanks of the joint teeth. Reference [8] used pneumatic devices in the bearing part of a jaw crusher system. During system operation, the pneumatic devices could press the movable half-bearing against the journal bearings to make them mesh with each other constantly, thus enabling the backlash to be eliminated. Reference [9] presented a new design for a single-roller enveloping hourglass worm gear. Through mathematical modeling, the study found that gear backlash could be eliminated by adjusting the radius of the roller and the base circle; the problems of teeth seizing and scuffing caused by zero backlash could also be avoided by using the roller's self-rotation property. References [10], [11] presented designs for different bearings that could eliminate the protective backlash and used these bearings in an active magnetic bearing system.

Electrical methods mainly use different methods to compensate for the nonlinear effects caused by backlash. References [12], [13] both used feedforward compensators to compensate for the backlash effect. Reference [14] added an offset to the output torque to compensate for and eliminate the distortion caused by backlash. Reference [15] used a compensation method based on ideal model control and designed a fuzzy controller with angle difference feedback. Reference [16] presented a switch control method in which time-optimal sliding mode control

The associate editor coordinating the review of this manuscript and approving it for publication was Qinfen Lu.

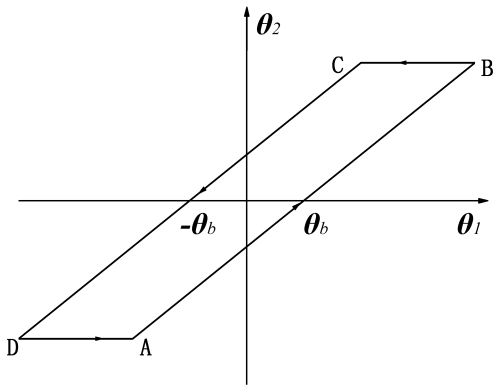

FIGURE 1. Mesh curve between the drive gear and the driven gear.

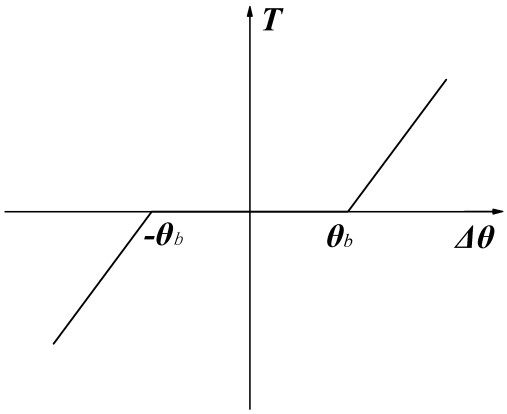

FIGURE 2. Torque curve between the drive gear and the driven gear.

was used when the system entered backlash and a nonlinear proportional-integral-derivative (PID) controller was used when the gears were meshed. References [17], [18] used statistical linearization methods to deal with the nonlinear characteristics caused by backlash. References [19]–[21] applied adaptive controllers based on different inputs to compensate for the errors caused by backlash.

The studies described above show that the mechanical methods to eliminate backlash effects often require additional complex processes in the gear transmission system, while the electrical methods require cumbersome algorithms. Along with the continuing improvements in microchip technology, the use of double motors to eliminate the effects of backlash has become a focus of research and numerous studies of this approach have been performed worldwide. In this article, a scheme that uses double motors and is based on a linearization approach is proposed. When compared with other research in this field, the scheme proposed here has no requirements for special components or processing, and it simplifies the control algorithm to allow the system's response speed and stability to be improved.

II. DYNAMIC MODEL OF THE SYSTEM

During gear system design, clearances are allowed to prevent clogging problems. These clearances may become enlarged as a result of processing and installation errors and the accuracy of the system's motion will be affected by the backlash from clearances of this type. When a drive gear meshes with a driven gear, the meshing curve is as shown in Fig. 1. The abscissa θ_1 shown in the figure is the drive gear's angular displacement, the ordinate θ_2 is the driven gear's angular displacement, and the clearance is $2\theta_b$. Lines AB and CD represent the motions during which the drive gear drives the driven gear to cause these gears to move together without backlash. Lines BC and DA represent the corresponding motions when the drive gear is operating in reverse. At this time, the driven gear did not mesh with the drive gear because of the backlash and had no displacement. Fig. 2 shows a simplified curve of the flexibility torque between two gears, in which the abscissa represents the relative angular displacement between the two gears, and the ordinate represents the flexibility torque. The figure shows that when the displacement is less than θ_b, there is no flexibility torque between the two gears, which means that the teeth of the drive gear are within range of the backlash and thus do not mesh with the driven gear.

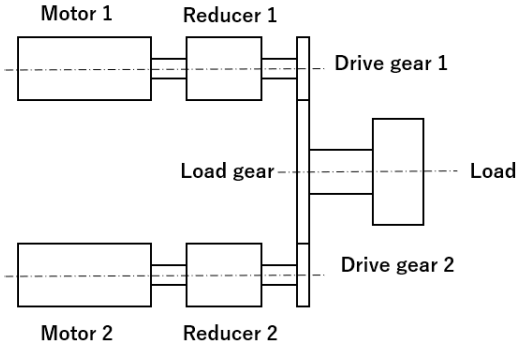

FIGURE 3. Principle of the two-motor system.

From the description above, it can be seen that the gear system motion with the backlash is a nonlinear motion and would thus affect the final system output.

To solve this problem, a backlash elimination scheme that uses double motors is proposed here. Fig. 3 illustrates the principle of the proposed scheme. This system uses two motors to drive two gears separately through two reducers; these two gears then both mesh with the load gear and drive it to drive the final load.

Without consideration of the backlash, the dynamic equations for the two-motor system can be written as:

$$\begin{cases} T_{e1} = \dfrac{3}{2} p_{n1} \psi_{f1} i_{q1} \\ T_{e2} = \dfrac{3}{2} p_{n2} \psi_{f2} i_{q2} \\ T_{c1} = i_{c1} T_{e1} - \left(i_{c1}^2 J_{m1} + J_{c1} \right) \ddot{\theta_{c1}} - \left(i_{c1}^2 b_{m1} + b_{c1} \right) \dot{\theta_{c1}} \\ T_{c2} = i_{c2} T_{e2} - \left(i_{c2}^2 J_{m2} + J_{c2} \right) \ddot{\theta_{c2}} - \left(i_{c2}^2 b_{m2} + b_{c2} \right) \dot{\theta_{c2}} \\ i_{m1} T_{c1} + i_{m2} T_{c2} = T_s + \left(J_d + J_l \right) \ddot{\theta_d} + \left(b_d + b_l \right) \dot{\theta_d} \end{cases} \tag{1}$$

where T_{e1} and T_{e2} [N·m] are the torques of the two motors, p_{n1} and p_{n2} are the pole numbers of the two motors, ψ_{f1} and ψ_{f2} [Wb] are the fluxes of the two motors, i_{q1} and i_{q2} [A] are the currents of the two motors, T_{c1} and T_{c2} [N·m] are the output torques of the two gears, i_{c1} and i_{c2} are the reduction ratios of the two reducers, J_{m1} and J_{m2} [kg·m^2] are the rotational inertias of the two motors, J_{c1} and J_{c2} [kg·m^2] are the rotational inertias of the two gears, θ_{c1} and θ_{c2} [rad] are the angular displacements of the drive gear and the driven gear respectively, b_{m1} and b_{m2} are the damping coefficients of the two motors, b_{c1} and b_{c2} are the damping coefficients of the two gears, i_{m1} and i_{m2} are the transmission ratios from the drive gears to the load gear, T_s [N·m] is the torque of the load, J_d [kg·m^2] is the rotational inertia of the load gear, J_l [kg·m^2] is the rotational inertia of the load, θ_d [rad] is the angular displacement of the load gear, b_d is the damping coefficient of the load gear, and b_l is the damping coefficient of the load.

Next, the backlash is brought into the system. The simplified model of the flexibility torque between the two drive gears and the load gear can be written as follows:

$$\begin{aligned} \phi_z &= \begin{cases} \theta_{cz} - i_{mz}\theta_d - \theta_b & \theta_{cz} - i_{mz}\theta_d \geq \theta_b \\ 0 & |\theta_{cz} - i_{mz}\theta_d| < \theta_b \\ \theta_{cz} - i_{mz}\theta_d + \theta_b & \theta_{cz} - i_{mz}\theta_d \leq -\theta_b \end{cases} \\ T_{cz} &= K_z\phi_z \quad z = 1, 2 \end{aligned} \tag{2}$$

where K_1 and K_2 are the flexibility torque coefficients between the two drive gears and the load gear.

If (2) is brought into (1), then the nonlinear model of the two-motor system with backlash can be built as shown in (3).

$$\begin{cases} T_{e1} = \dfrac{3}{2} p_{n1}\psi_{f1} i_{q1} \\ T_{e2} = \dfrac{3}{2} p_{n2}\psi_{f2} i_{q2} \\ T_{c1} = K_1\Phi_1 = i_{c1}T_{e1} - \left(i_{c1}^2 J_{m1} + J_{c1}\right)\ddot{\theta_{c1}} \\ \qquad\qquad - \left(i_{c1}^2 b_{m1} + b_{c1}\right)\dot{\theta_{c1}} \\ T_{c2} = K_2\Phi_2 = i_{c2}T_{e2} - \left(i_{c2}^2 J_{m2} + J_{c2}\right)\ddot{\theta_{c2}} \\ \qquad\qquad - \left(i_{c2}^2 b_{m2} + b_{c2}\right)\dot{\theta_{c2}} \\ i_{m1}K_1\Phi_1 + i_{m2}K_2\Phi_2 = T_s + (J_d + J_l)\ddot{\theta_d} + (b_d + b_l)\dot{\theta_d} \end{cases} \tag{3}$$

III. CONTROL MODEL OF THE SYSTEM

In real applications of normal turntable system, the drive gears that are driven by the motors will enter a nonlinear region because of the backlash between the drive gear and the load gear; this will mean that the load gear shaft's output cannot maintain a linear relationship with the motor's output, which will finally lead to a reduction in the stability of the system output. When the two-motor system is operational, a torque command will be calculated and will subsequently be decomposed into two commands to be sent to the motor controller. If a control strategy can be designed to decompose the torque command in a reasonable manner, then the two drive gears would be able to enter the nonlinear region separately. There will then be at least one drive gear meshing with the load gear at any time. This new system would be equivalent to a single-motor system without backlash, which means that linear control could then be realized.

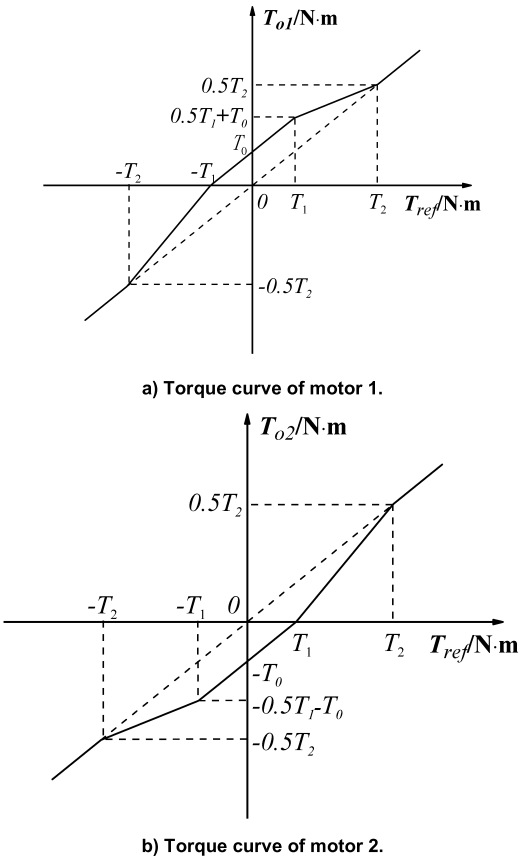

FIGURE 4. Bias torque curves of the two motors.

The state variables that describe the proposed system include the angular displacements and the angular velocities of the two motors and the load gear shaft. Equation (4) represents the state vector of the system:

$$X(t) = [\theta_d\ \omega_d\ \theta_{m1}\ \omega_{m1}\ \theta_{m2}\ \omega_{m2}]^T \tag{4}$$

where $X(t)$ is the system state vector, θ_d [rad] is the angular displacement of the load gear shaft, ω_d [rad/s] is the angular velocity of the load gear shaft, θ_{m1} [rad] is the angular displacement of motor 1, ω_{m1} [rad/s] is the angular velocity of motor 1, θ_{m2} [rad] is the angular displacement of motor 2, and ω_{m2} [rad/s] is the angular velocity of motor 2.

In this work, the two motors, the two reducers, and the two drive gears are supposed to have same characteristic, thus allowing the system damping to be ignored. According to the law of rotation, the relationship between rotor's angular acceleration $\dot{\omega}$, rotor's rotational inertia J and motor's output torque T can be written as:

$$\dot{\omega} = \frac{T}{J} \tag{5}$$

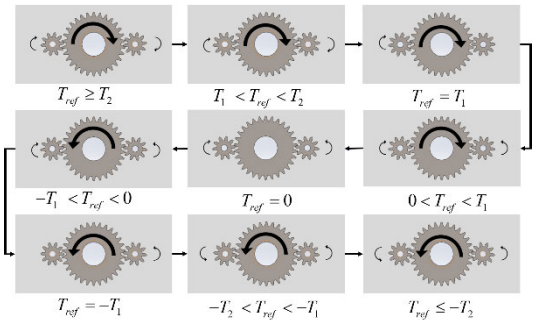

FIGURE 5. Schematic diagram of the turning process.

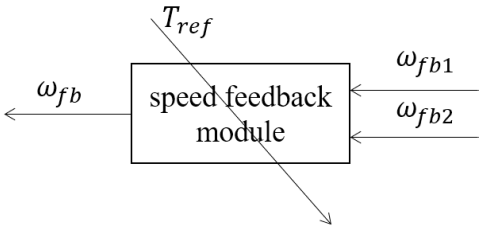

FIGURE 6. Schematic of the feedback switching module.

The system's state equations can then be written as:

$$\begin{cases} \dot{\theta_d} = \omega_d \\ \dot{\omega_d} = \dfrac{f_d\left(T_{c1}, T_{c2}, i_m\right) - T_s}{J_d + J_l} \\ \dot{\theta_{m1}} = \omega_{m1} \\ \dot{\omega_{m1}} = \dfrac{f_1\left(T_{e1}, T_{c1}, i_c\right)}{J_m i_c + J_c / i_c} \\ \dot{\theta_{m2}} = \omega_{m2} \\ \dot{\omega_{m2}} = \dfrac{f_2\left(T_{e2}, T_{c2}, i_c\right)}{J_m i_c + J_c / i_c} \end{cases} \tag{6}$$

where $f_d\left(T_{c1}, T_{c2}, i_m\right)$ [N·m] is the torque function of the load gear shaft, $f_1\left(T_{e1}, T_{c1}, i_c\right)$ [N·m] is the torque function from motor 1 to drive gear 1, $f_2\left(T_{e2}, T_{c2}, i_c\right)$ [N·m] is the torque function from motor 2 to drive gear 2, i_c is the reduction ratio of the reducer, and J_c [kg·m^2] is the rotational inertia of the drive gear.

The torque of the load gear shaft is the sum of the output torques from the two drive gears, and the torques of the drive gears are the differences between the outputs of the motors and the reaction torques from the load gear. The torque function can then be written as:

$$\begin{cases} f_d = i_m T_{c1}\left(\theta_d, \theta_{m1}, \theta_b, i_m, i_c, K\right) \\ \qquad + i_m T_{c2}\left(\theta_d, \theta_{m2}, \theta_b, i_m, i_c, K\right) \\ f_1 = i_c T_{e1}\left(T_{ref}\right) - T_{c1}\left(\theta_d, \theta_{m1}, \theta_b, i_m, i_c, K\right) \\ f_2 = i_c T_{e2}\left(T_{ref}\right) - T_{c2}\left(\theta_d, \theta_{m2}, \theta_b, i_m, i_c, K\right) \end{cases} \tag{7}$$

where $T_{c1}\left(\theta_d, \theta_{m1}, \theta_b, i_{m1}, i_c, K\right)$ [N·m] is the torque function from drive gear 1 to the load gear, $T_{c2}\left(\theta_d, \theta_{m2}, \theta_b, i_{m2}, i_c, K\right)$ [N·m] is the torque function from drive gear 2 to the load gear, $T_{e1}\left(T_{ref}\right)$ [N·m] is the output torque from motor 1, $T_{e2}\left(T_{ref}\right)$ [N·m] is the output torque from motor 2, and K is the flexibility torque coefficient of the gears.

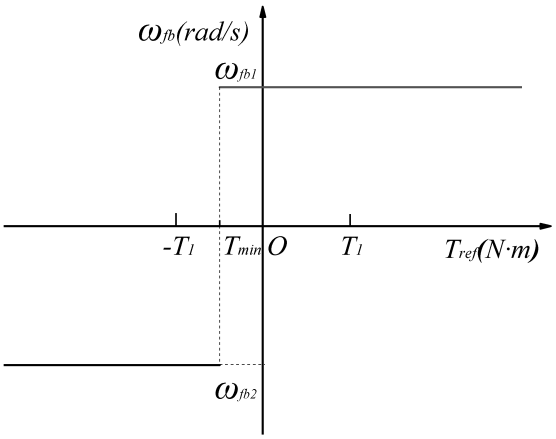

FIGURE 7. Schematic diagram of the speed switching process.

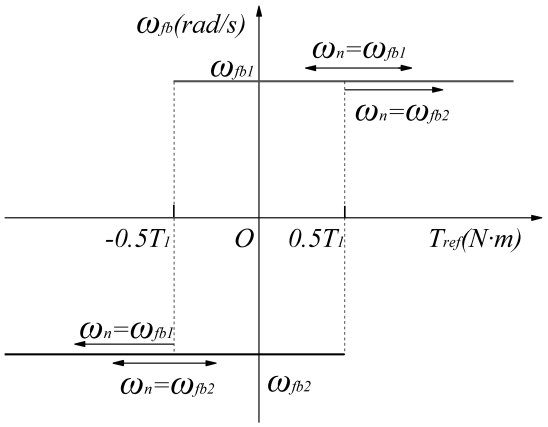

FIGURE 8. Switching curve with reference to the feedback speed.

Because of the existence of the backlash, both T_{c1} and T_{c2} are nonlinear and their values are dependent on both the backlash and the relative angles between the drive gears and the load gear. These relative angles can be calculated using (8):

$$\begin{cases} \Delta\theta_1 = \theta_{m1}/i_c - \theta_d i_m \\ \Delta\theta_2 = \theta_{m2}/i_c - \theta_d i_m \end{cases} \tag{8}$$

where $\Delta\theta_1$ [rad] is the relative angle between drive gear 1 and the load gear, and $\Delta\theta_2$ [rad] is the relative angle between drive gear 2 and the load gear.

The mesh torque direction between the drive gear and the load gear is set as the forward direction when $\Delta\theta_1 - \theta_d > 0$ and $\Delta\theta_2 - \theta_d > 0$. Motor 1 is set to provide the forward torque and motor 2 is set to provide the backward torque when the two motors provide opposite torques. If (3) is brought into (7), then (7) could be divided into the five linear situations shown below based on the system's working processes.

1) System runs in forward direction. The two drive gears mesh with the load gear in the forward direction.

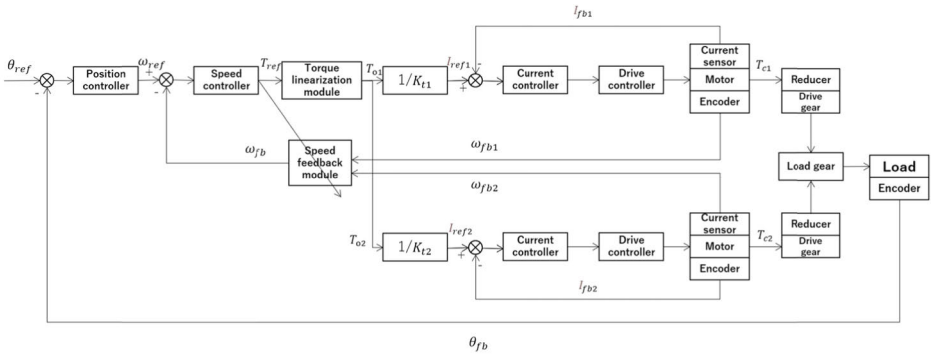

FIGURE 9. Control block diagram of the two-motor system.

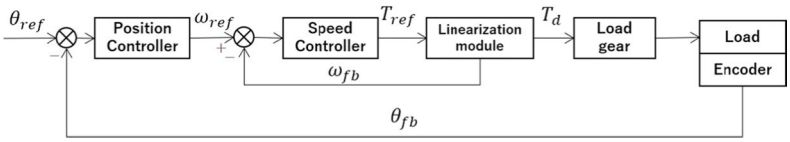

FIGURE 10. Equivalent block diagram of the two-motor system.

This system is a linear system. The torques are then calculated using (9):

$$\begin{cases} f_d = i_m K\left(\left(\theta_{m1}+\theta_{m2}\right)/i_c - 2i_m\theta_d - 2\theta_b\right) \\ f_1 = i_c T_{e1} - K\left(\theta_{m1}/i_c - i_m\theta_d - \theta_b\right) \\ f_2 = i_c T_{e2} - K\left(\theta_{m2}/i_c - i_m\theta_d - \theta_b\right) \end{cases} \tag{9}$$

2) System begins to change direction to backward. At this time, motor 1 still outputs a forward torque, but motor 2 begins to output a backward torque. Drive gear 1 meshes with the load gear in the forward direction, but drive gear 2 does not mesh with the load gear. The system then turns into a linear gear transmission system driven by motor 1 and a system with motor 2. The torques are then calculated using (10):

$$\begin{cases} f_d = i_m K\left(\theta_{m1}/i_c - i_m\theta_d - \theta_b\right) \\ f_1 = i_c T_{e1} - K\left(\theta_{m1}/i_c - i_m\theta_d - \theta_b\right) \\ f_2 = i_c T_{e2} \end{cases} \tag{10}$$

3) System is still in the process of changing direction. Drive gear 1 meshes with the load gear in the forward direction and drive gear 2 meshes with the load gear in the backward direction. This system is a linear system. The torques can then be calculated using (11):

$$\begin{cases} f_d = i_m K\left(\left(\theta_{m1}+\theta_{m2}\right)/i_c - 2i_m\theta_d\right) \\ f_1 = i_c T_{e1} - K\left(\theta_{m1}/i_c - i_m\theta_d - \theta_b\right) \\ f_2 = i_c T_{e2} - K\left(\theta_{m2}/i_c - i_m\theta_d + \theta_b\right) \end{cases} \tag{11}$$

4) System finishes changing direction and begins to run backward. At this time, motor 1 begins to output a backward torque. Drive gear 1 does not mesh with the load gear, but drive gear 2 meshes with the load gear in the backward direction. The system then turns into a linear gear transmission system driven by motor 2 and a system with motor 1. The torques can then be calculated using (12):

$$\begin{cases} f_d = i_m K\left(\theta_{m1}/i_c - i_m\theta_d + \theta_b\right) \\ f_1 = i_c T_{e1} \\ f_2 = i_c T_{e2} - K\left(\theta_{m2}/i_c - i_m\theta_d + \theta_b\right) \end{cases} \tag{12}$$

5) System runs in the backward direction. The two drive gears mesh with the load gear in the backward direction. This system is a linear system. The torques can then be calculated using (13):

$$\begin{cases} f_d = i_m K\left(\left(\theta_{m1}+\theta_{m2}\right)/i_c - 2i_m\theta_d + 2\theta_b\right) \\ f_1 = T_{e1} i_c - K\left(\theta_{m1}/i_c - i_m\theta_d + \theta_b\right) \\ f_2 = T_{e2} i_c - K\left(\theta_{m2}/i_c - i_m\theta_d + \theta_b\right) \end{cases} \tag{13}$$

The equations above illustrate that the torque algorithm can be designed to maintain the system in these five states throughout the entire working process, thus allowing the system output to be controlled in a linear manner.

IV. LINEARIZATION CONTROL METHOD FOR THE SYSTEM

A. LINEARIZATION TORQUE CONTROL METHOD FOR THE SYSTEM

To realize the five states described in the previous section, bias torques must be imposed on the two drive gears during system booting and reversal to ensure that one motor provides dynamic torque while the other provides a resistance torque. After system booting or reversal, the bias torques will then be canceled and both motors will then provide dynamic torques to drive the system.

In this work, two inflection points are set in the algorithm to increase the motor efficiencies and prevent uneven stressing

of the load gear. Fig. 4 shows the bias torque curves of the two motors. Equation (14) is used to calculate the command torque.

$$T_{o1} = \begin{cases} \frac{T_{ref}}{2} & T_{ref} \le -T_2 \\ \frac{T_2}{2(T_2-2T_0)}T_{ref} + \frac{T_0T_2}{T_2-2T_0} & -T_2 < T_{ref} < -T_1 \\ \frac{T_{ref}}{2} + T_0 & -T_1 \le T_{ref} \le T_1 \\ \frac{T_2-4T_0}{2(T_2-2T_0)}T_{ref} + \frac{T_0T_2}{T_2-2T_0} & T_1 < T_{ref} < T_2 \\ \frac{T_{ref}}{2} & T_{ref} \ge T_2 \end{cases}$$

$$T_{o2} = \begin{cases} \frac{T_{ref}}{2} & T_{ref} \le -T_2 \\ \frac{T_2-4T_0}{2(T_2-2T_0)}T_{ref} - \frac{T_0T_2}{T_2-2T_0} & -T_2 < T_{ref} < -T_1 \\ \frac{T_{ref}}{2} - T_0 & -T_1 \le T_{ref} \le T_1 \\ \frac{T_2}{2(T_2-2T_0)}T_{ref} - \frac{T_0T_2}{T_2-2T_0} & T_1 < T_{ref} < T_2 \\ \frac{T_{ref}}{2} & T_{ref} \ge T_2 \end{cases} \quad (14)$$

where T_{ref} [N·m] is the command torque of the system, T_{o1} [N·m] is the command torque of motor 1, T_{o2} [N·m] is the command torque of motor 2, T_0 [N·m] is the bias torque, T_1 [N·m] is the torque on the first inflection point, and T_2 [N·m] is the torque on the second inflection point.

T_1 and $-T_1$ are the intersection points of the constant bias torque curve and the graded bias torque curve, and T_2 and $-T_2$ are the intersection points of the graded bias torque curve and the zero-bias torque curve, respectively. When no bias torque is imposed, the torque curve is then directly proportional; when the absolute value of T_{ref} lies between the absolute values of T_1 and T_2, the bias torque will then change gradually; and when the absolute value of T_{ref} is smaller than the absolute value of T_1, the bias torque is then equal to T_o.

Due to the two motor systems have same characteristic, torque command will be decomposed evenly on two motors, which means $T_{o1} = T_{o2} = \frac{T_{ref}}{2}$ and the slope of torque curve is 0.5 when no bias torque is imposed. When $-T_1 \le T_{ref} \le T_1$, constant bias torque T_o is imposed, the slope of torque curve in this interval should still be 0.5, which means $T_1 = 2T_o$. If T_o and T_2 can be determined, then the curve can also be determined. These parameters are empirical values and must be adjusted based on the working conditions to obtain the best possible performance during practical operation. Preliminarily, T_o is set at 5% of the rated torque and T_2 is set at 35% of the rated torque, then the value of T_1 is 10% of the rated torque.

The backlash mainly appears during the system booting and reversal processes. Fig. 5 shows a schematic diagram

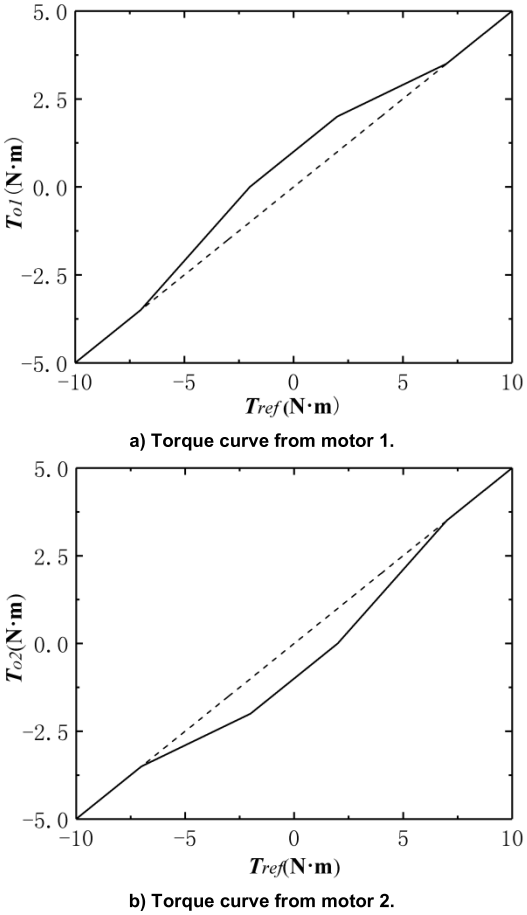

FIGURE 11. Torque curves after the linearization module.

of the process that occurs when the system is reversing from operation in the forward direction toward the backward direction.

Initially, the system runs in the forward direction, where $T_{ref} \ge T_2$ and both motors output dynamic torque of $\frac{T_{ref}}{2}$, both drive gears mesh with the load gear in the forward direction, and there is no bias torque. Then, when the system begins to reverse, T_{ref} begins to decrease until $T_1 < T_{ref} < T_2$; the two motors then begin to impose the bias torque, motor 2 begins to reverse, the two drive gears still mesh with the load gear, and the system still runs in the forward direction but is decelerating. When T_{ref} decreases to $T_{ref} = T_1$, motor 2 then outputs zero torque and its drive gear disengages from the load gear; motor 1's drive gear drives the load gear forward by itself, and the system decelerates in the forward direction. When T_{ref} decreases to $0 < T_{ref} < T_1$, motor 1 then outputs the dynamic torque and its gear meshes positively with the load gear, whereas motor 2 outputs the resistance torque and its gear meshes negatively with the load gear. When T_{ref} decreases to 0, motors 1 and 2 output equal torques but in opposite directions and the system is stopped. T_{ref} then continues decreasing until $-T_1 < T_{ref} < 0$; motor 1 begins to reverse and its output torque begins to reduce, but the gear still meshes with forward load gear and

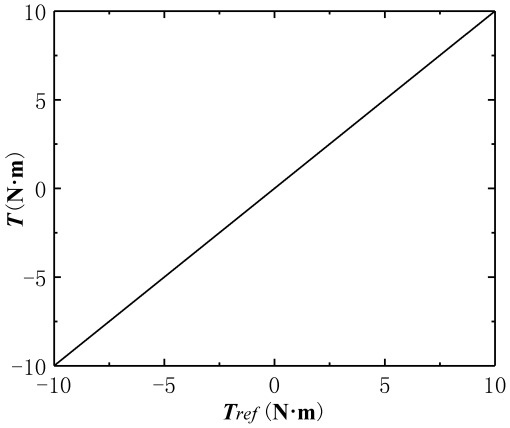

a) Sum of the output torques of the two motors.

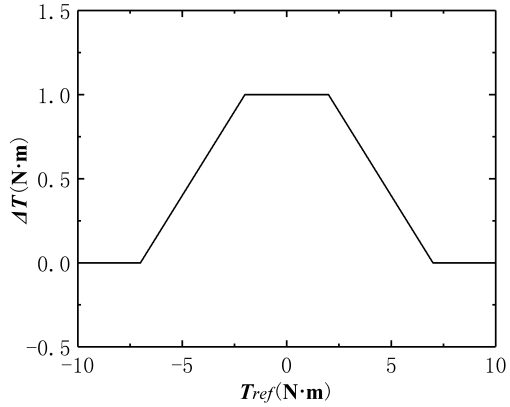

b) Difference between the two torques.

FIGURE 12. Sum and difference characteristics of the torques of the two motors.

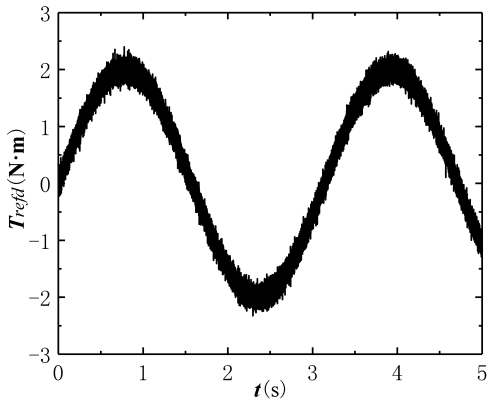

FIGURE 13. Input signal to the speed module.

the system begins to start reversing. Then, when $T_{ref} = -T_1$, motor 1 outputs zero torque and its gear disengages from the load gear; motor 2's gear alone then drives the load gear backward and the system accelerates backward. When $-T_2 < T_{ref} < -T_1$, both motors' gears engage the load gear backward and drive the system to run backward, and the bias torque begins to reduce. When $T_{ref} < -T_2$, both bias torques decrease to zero, both motors output a dynamic torque of $-\frac{T_{ref}}{2}$, both drive gears mesh with the load gear in

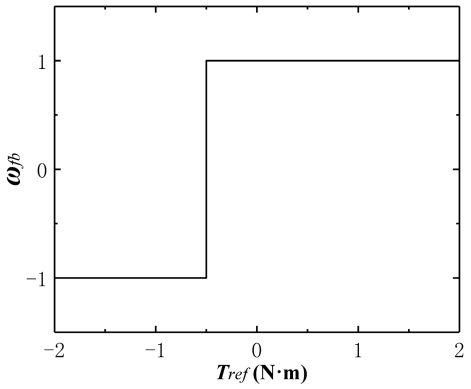

a) Judgment curve.

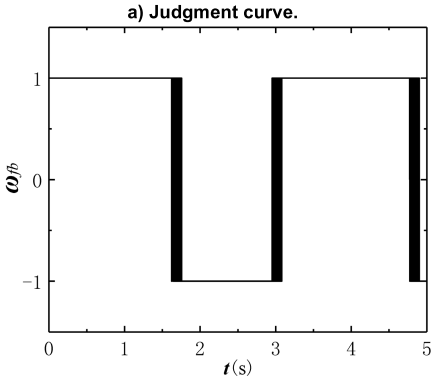

b) Switching output.

FIGURE 14. Switching results obtained when only one switching point is used.

the backward direction, and the system reversal is complete. When the system turns back from the reverse direction toward the forward direction, the process will be similar but opposite to that described above.

B. LINEARIZATION METHOD FOR THE SPEED FEEDBACK

The two motors have equivalent rotational speeds and maintain a linear relationship with the load gear shaft speed at most points during system operation. Therefore, the system could use a single speed loop and the speed of one motor to provide the feedback required to control both motors, thus allowing the control algorithm to be simplified. However, when the system is either booting or reversing, the gear of one of the two motors will disengage from the load gear because of the effect of the backlash, and its speed thus cannot reflect the motion state of the load gear shaft in that case. If this motor's speed is used to provide the feedback, the system's output accuracy and stability will both be reduced. To resolve this problem, a speed feedback module is designed that can switch the feedback between motors 1 and 2 when required. When the gear on motor 1 disengages from the load gear, the speed of motor 2 will then be switched to be used to provide the feedback, and vice versa. Fig. 6 shows a schematic diagram of this module.

The module has two input signals: one conditional judgment signal and one output signal. The torque command T_{ref}

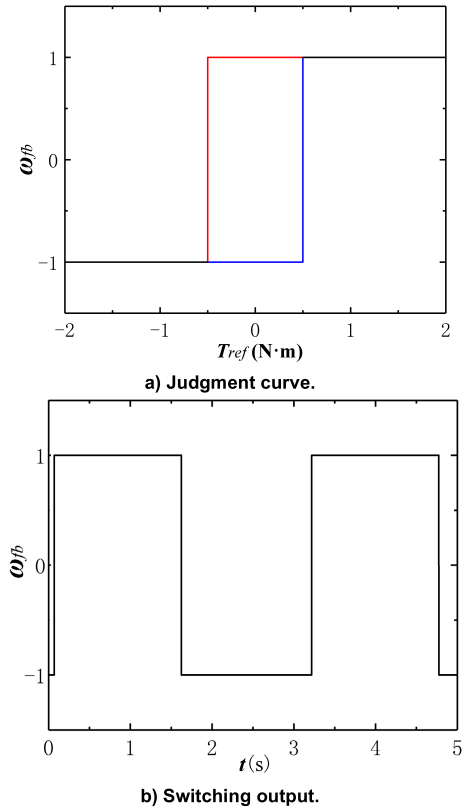

FIGURE 15. Switching results obtained when two switching points are used.

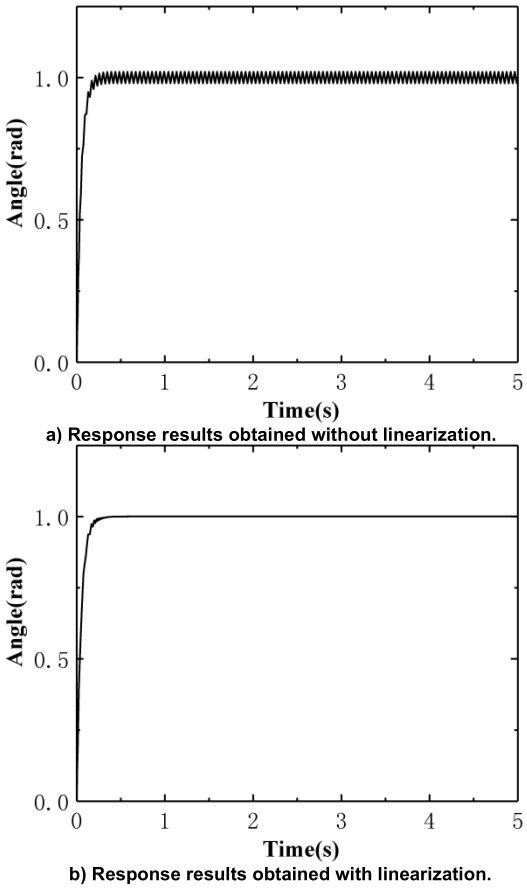

FIGURE 16. Response curves for the step position command.

from the speed controller is used to determine the situation of the two motors. When the output obtained from motor 1 is reduced to be close to zero, the feedback speed of motor 2 ω_{fb2} is then switched to be used as the loop feedback speed ω_{fb}, and vice versa. A schematic diagram of the speed switching process is shown in Fig. 7. T_{min} is used as the switching point in this case.

The switching formula is given by (15):

$$\omega_{fb} = \begin{cases} \omega_{fb1} & T_{ref} \geq T_{min} \\ \omega_{fb2} & T_{ref} < T_{min} \end{cases} \tag{15}$$

where ω_{fb} [rad/s] is the speed feedback from the system, ω_{fb1} [rad/s] is the speed feedback from motor 1, ω_{fb2} [rad/s] is the speed feedback from motor 2, and T_{min} [N·m] is the switching condition value of the system torque. To cause switching to occur before the system torque decreases to zero, the conditions $T_{min} \neq 0$ and $-T_1 < T_{min} < T_1$ are required.

In practical applications, the torque commands may be subject to fluctuations caused by system disturbances. If the torque command T_{ref} fluctuates near T_{min}, the feedback will then switch repeatedly between the signals from motor 1 and motor 2 at high frequency, which will lead to reduced system stability. To solve this problem, the previous control cycle's speed feedback ω_n is also used as the switching condition. To simplify the control program required, the T_{min} value is set at $\pm 0.5T_1$, The switching formula is then given by:

$$\omega_{fb} = \begin{cases} \omega_{fb1} & T_{ref} \geq -0.5T_1 \& \omega_n = \omega_{fb1} \\ \omega_{fb2} & T_{ref} < -0.5T_1 \& \omega_n = \omega_{fb1} \\ \omega_{fb2} & T_{ref} \leq 0.5T_1 \& \omega_n = \omega_{fb2} \\ \omega_{fb1} & T_{ref} > 0.5T_1 \& \omega_n = \omega_{fb2} \end{cases} \tag{16}$$

The switching curve is then as shown in Fig. 8.

If the torque command is greater than $0.5T_1$, then ω_{fb1} from motor 1 will always be used as the feedback, regardless of the feedback that was used in the previous cycle; however, if the torque command is in the range between $0.5T_1$ and $-0.5T_1$, the feedback that was used in the previous cycle will then be used as the feedback and no switching will occur; finally, if the torque command is less than $-0.5T_1$, then ω_{fb2} from motor 2 will always be used as the feedback, regardless of the feedback that was used in the previous cycle.

If the torque command changes from positive to negative, then ω_{fb1} will continue to be used as the feedback until the torque command nears $-0.5T_1$. When the torque command is less than $-0.5T_1$, the cycle will then use ω_{fb2} as the feedback and the system will not switch feedback again, even if the command exceeds $-0.5T_1$, because of the fluctuations caused by the disturbance. When the torque command changes from negative to positive, the process is

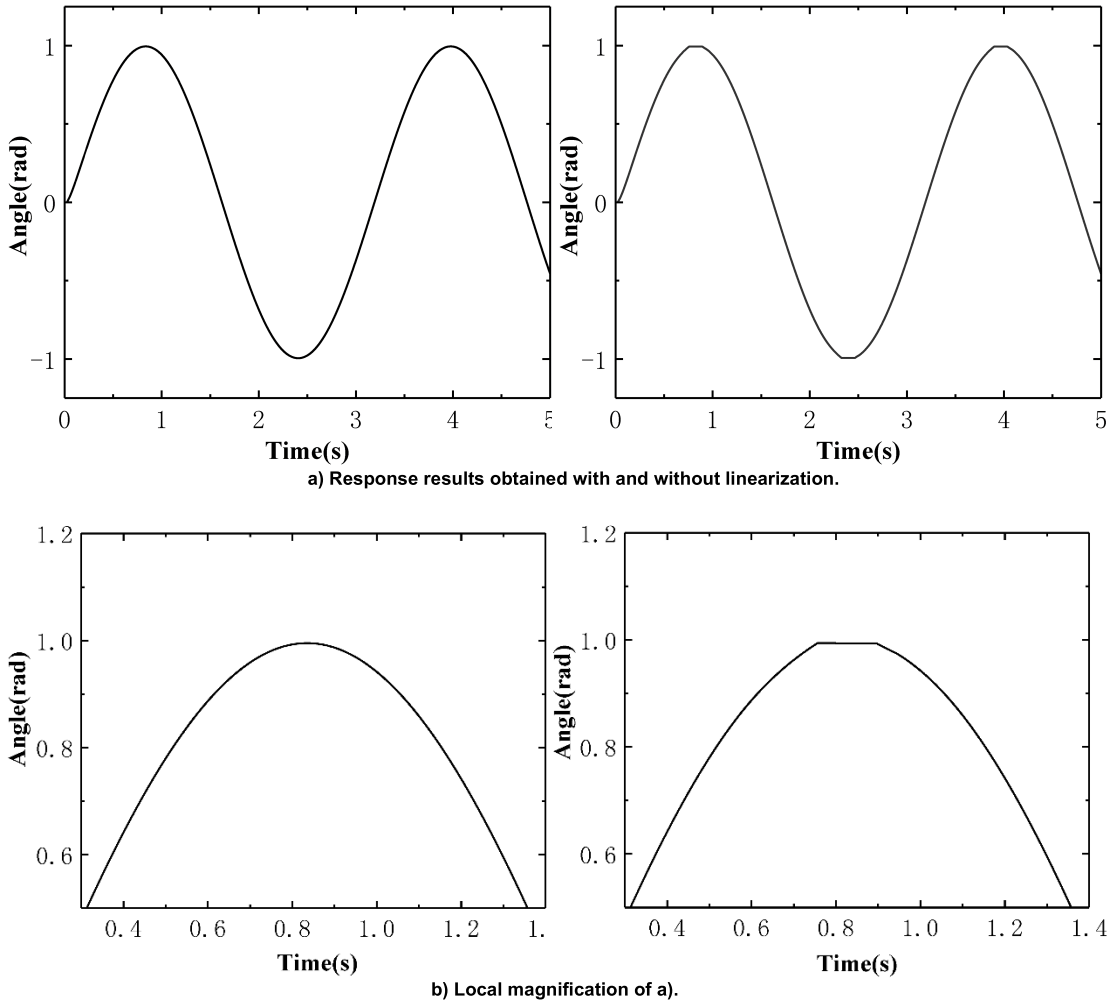

FIGURE 17. Response curves for the sinusoidal position command.

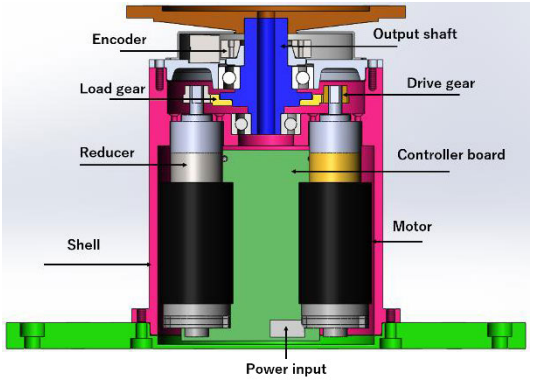

FIGURE 18. Turntable structure.

similar: ω_{fb2} will continue to be used as the feedback until the torque command nears $0.5T_1$; then, when the command is greater than $0.5T_1$, the cycle will continue to use ω_{fb1} as the feedback and will not switch the feedback again. Throughout this process, there will be only one switching operation when the command reaches the switching point, and it will not be affected by disturbances.

After implementation of the process described above, the speed of the load gear shaft can then be controlled linearly. The linear relationship between the feedback speed and the load gear shaft speed can be given as shown in (17).

$$\omega_{fb} = i_c i_m \omega_d \tag{17}$$

A block diagram of the proposed control system is shown in Fig. 9. This system includes a position controller, a speed controller, a torque linearization module, a speed feedback linearization module, a current controller, a gear transmission system, and encoders. PI control method is used in all three controllers, and the control parameter are adjusted manually during debugging process. When system works, the position command is transmitted from the host computer and its difference value when compared with the position feedback is sent to the position controller. The position controller calculates the required speed command and the difference between this speed command and the speed feedback from the linearization module is then sent to the speed controller. The speed controller then calculates the torque command and sends it to the torque linearization module; the decomposed torques are subsequently output from the two motors separately to drive

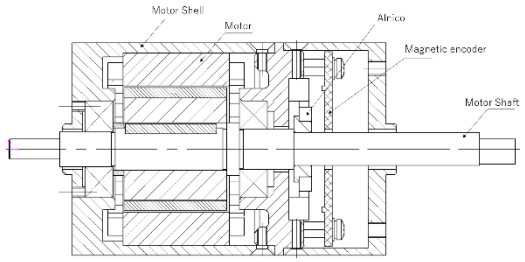

FIGURE 19. Servo motor structure.

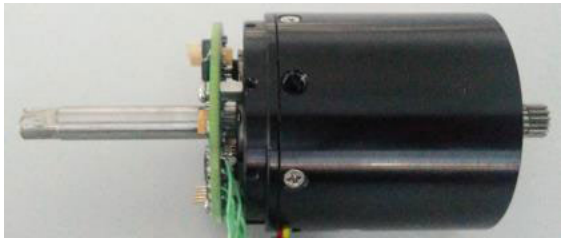

FIGURE 20. Photograph of the servo motor.

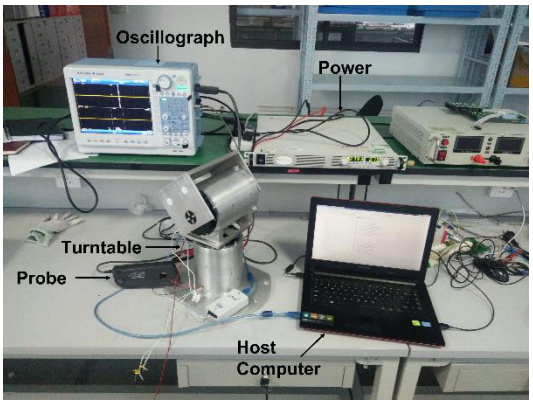

FIGURE 21. Experimental platform.

the two drive gears to mesh with the load gear and thus drive the gear.

Use of these linearization modules allows the two-motor system to be equivalent to the single-motor linear system without backlash shown in Fig. 10. A nonlinear system with backlash could then realize linear control of the load gear.

V. SIMULATION OF THE SYSTEM

First, the torque linearization module and the speed feedback linearization module are simulated to verify their effectiveness. The rated torque is set at 20 N·m and the torque command increases from −20 N·m to 20 N·m; under these conditions, the bias torque is then 1 N·m, the torque on the first inflection point T_1 is 2 N·m, and the torque on the second inflection point T_2 is 7 N·m, as mentioned previously. Fig. 11 shows the torque curves for the two motors after the linearization module. In both cases, the solid curve is the torque curve after linearization and the dotted curve is the torque command before linearization. Fig. 12 shows the sum and difference curves for the output torques from the two motors.

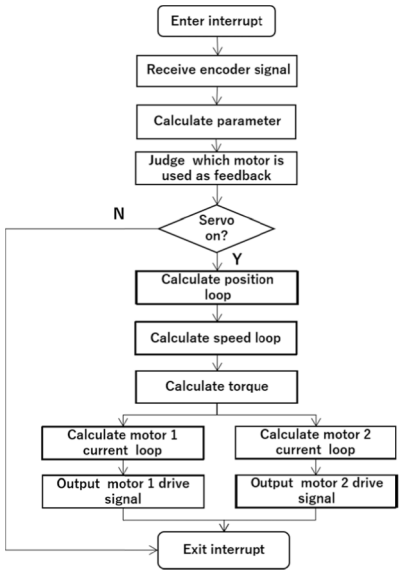

FIGURE 22. Control process flow chart for the two-motor system.

The curve shape shown in Fig. 11 is the same as that of the designed curve shown in Fig. 4. Figure 12(a) shows that the final torque is the same as the command torque obtained from the controller, figure 12(b) shows that when the absolute value of the command torque T_{ref} is greater than the absolute value at the inflection point, the two motors will then output equivalent torques; when T_{ref} is smaller than the torque at the inflection point, the bias torque will then be imposed to eliminate the effects of the backlash.

To simulate the speed feedback linearization module, noise is introduced to the system. The range for the sinusoidal torque command is set from −2 N·m to 2 N·m, and the noise amplitude is less than 0.5 N·m. The curve obtained for the input signal is shown in Fig. 13.

This curve is then input to the speed feedback linearization module to simulate switching of the feedback. The module then outputs the selection result, where an output of 1 means that motor 1's feedback is selected and an output of −1 means that motor 2's feedback is selected. First, the single switch condition torque value is set at −0.5 N·m and the result is then as shown in Fig. 14. The figure shows that repeated switching would occur with high frequency when the torque command fluctuates near the switching point because of the noise in the system.

When the double switching condition torque value is set at ±0.5 N·m, the results are as shown in Fig. 15. If motor 1's feedback was used in the previous cycle, then the red curve will be used to perform the judgment; however, if motor 2's feedback was used in the previous cycle, then the blue curve will be used to perform the judgment. The figure shows that the repeated switching problem has now been eliminated.

A step position command and a sinusoidal position command are then input to simulate the complete system. Fig. 16 shows the results that were obtained for the step command with and without linearization. The figure indicates that the output signal obtained without linearization

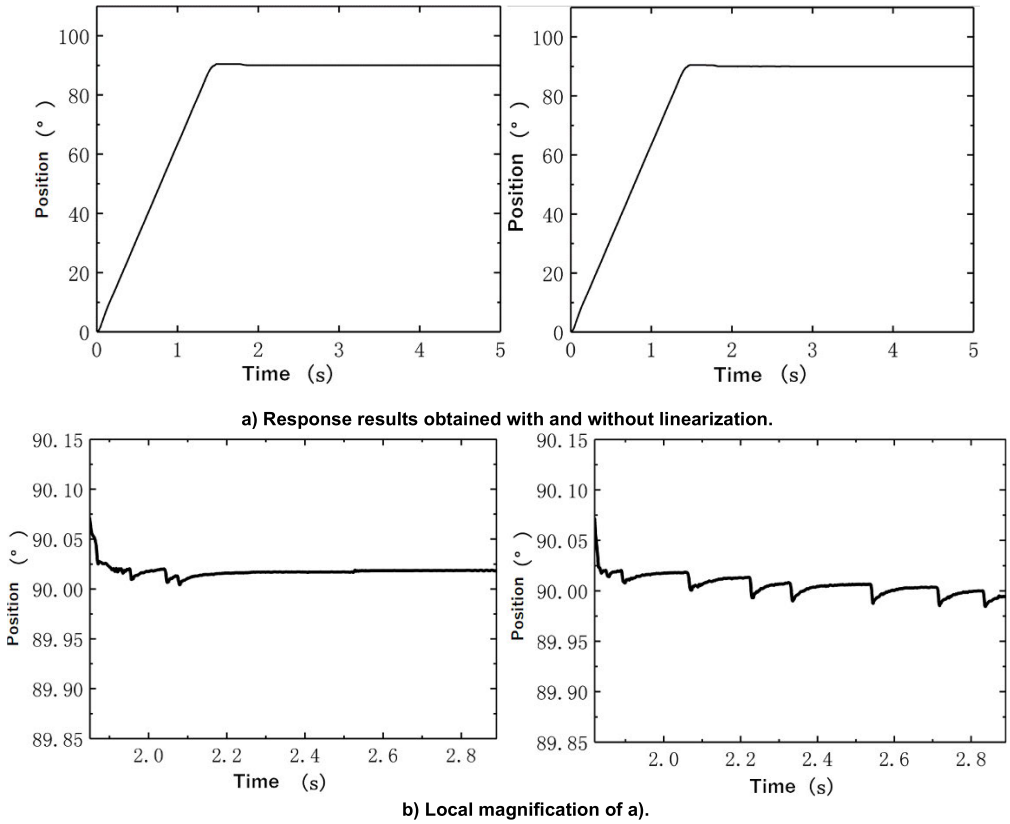

FIGURE 23. Results obtained for the system with and without the linearization algorithm.

contains jitter due to the backlash. In contrast, the output signal obtained with linearization is stable because equivalent bias torques acting in opposing directions are imposed on the two drive gears, causing them to mesh with the load gear and thus eliminate the backlash when the load gear reaches the command position.

Figure 17 shows the results that were obtained for the sinusoidal command with and without linearization. The curve obtained without linearization is cut at the top, which means that the backlash causes distortion of the system motion when the system is reversing. In contrast, the linearization algorithm eliminates the backlash, which means that the curve obtained with linearization shows zero distortion.

The simulation results show that the linearization module can resolve the backlash problem that occurs during system booting and reversal by imposing appropriate bias torques on the two drive gears using the two motors.

VI. EXPERIMENT

The structures of the turntable and the motor that were used in the experiments are illustrated in Figs. 18 and 19, respectively.

Fig. 20 shows a photograph of the actual servo motor and Fig. 21 shows a photograph of the experimental platform used.

The control process flow chart is shown in Fig. 22. The encoder signals are received initially and the motor to be used for the feedback is then selected. When the servo motor is started, the speed command is calculated using the position loop and this command is then sent to the speed loop; the torque command is then calculated using the speed loop and this command is then sent to the linearization module. Two torque commands are calculated for the two servo motors and these commands are sent to the two independent current loops; two groups of pulse width modulation (PWM) signals are then output to the motors for the driving process.

A 90° position command was input into the system for the experiment. The cases without and with use of the linearization algorithm were tested separately and the results obtained are shown in Figs. 23.

The results presented above demonstrate that when the linearization algorithm was not used, the system oscillated after completion of the location process because of the backlash that occurred between the gears; however, when the linearization algorithm was used, the system remained stable after the location process because two equal torques acting in opposing directions were still imposed on the load gear.

VII. CONCLUSION

In this article, a backlash elimination scheme based on linearization using a double motor system is proposed to solve the oscillation problem that occurs in turntable systems because of backlash in the reducer gear transmission. First, a dynamic model of the two-motor system with backlash is

constructed. The control model is then built and the nonlinear system with backlash is transformed into a linear system by providing two torques that act in opposing directions from the two motors. The torque calculation method is then designed, and a speed feedback module is proposed that prevents the system from using the speed from a motor with a gear that has disengaged from the load gear as a feedback signal. Finally, the system is simulated and tested, and the results verify the effectiveness of the proposed scheme. After application of the linearization algorithm, the system oscillations are reduced, and the system can then remain stable after the location process is completed. The torque distribution scheme in this manuscript is mainly focus on the turning process and suitable for rapid locating system. For continuous rotation system, a new torque distribution method is needed to solve the backlash elimination problem during dynamic acceleration or deceleration process.

REFERENCES

[1] C. I. Park, "Dynamic behavior of the spur gear system with time varying stiffness by gear positions in the backlash," *J. Mech. Sci. Technol.*, vol. 34, no. 2, pp. 565–572, Feb. 2020.

[2] F. Yang, G. Liu, H. Yu, Y. Cao, and K. He, "Rigid-flexible coupling dynamic simulation of precision reducer with backlash," in *Proc. 6th Int. Conf. Mech., Automot. Mater. Eng. (CMAME)*, Hong Kong, Aug. 2018, pp. 85–89.

[3] T. Yang, S. Yan, W. Ma, and Z. Han, "Joint dynamic analysis of space manipulator with planetary gear train transmission," *Robotica*, vol. 34, no. 5, pp. 1042–1058, May 2016.

[4] H. Zhang, J. Wang, S. Wang, S. Wang, and G. He, "A comparative investigation of meshing characteristics of anti-backlash single-and double-roller enveloping hourglass worm gears," *J. Adv. Mech. Des., Syst., Manuf.*, vol. 13, no. 3, pp. 1881–3054. Aug. 2019.

[5] X. Chu, H. Xu, X. Wu, J. Tao, and G. Shao, "The method of selective assembly for the RV reducer based on genetic algorithm," *Proc. Inst. Mech. Eng., C, J. Mech. Eng. Sci.*, vol. 232, no. 6, pp. 921–929, Mar. 2018.

[6] T. Li, X. An, X. Deng, J. Li, and Y. Li, "A new tooth profile modification method of cycloidal gears in precision reducers for robots," *Appl. Sci.*, vol. 10, no. 4, p. 1266, Feb. 2020.

[7] G. Stan, "Backlash decrease system of reducers/gearboxes in feed kinematical linkage structure of CNC machine tools," in *Proc. IOP Conf., Mater. Sci. Eng.*, Aug. 2016, vol. 145, no. 5, Art. no. 052009.

[8] A. G. Nikitin, A. V. Abramov, I. A. Bazhenov, and V. V. Dorofeev, "Investigation of the jaw crusher operation with backlash eliminators," in *Proc. IOP Conf.: Earth Environ. Sci.*, Jul. 2021, vol. 823, no. 1, Art. no. 012025.

[9] X. Deng, J. Wang, S. Wang, S. Wang, J. Wang, S. Li, Y. Liu, and G. He, "Investigation on the backlash of roller enveloping hourglass worm gear: Theoretical analysis and experiment," *J. Mech. Des.*, vol. 141, no. 5, May 2019, Art. no. 053302.

[10] C. Yu, Y. Sun, H. Wang, F. Shi, Y. Chen, and W. Shan, "Influence of conical degree on the performance of radial and axial integrated auxiliary bearing for active magnetic bearing system," *J. Mech. Sci. Technol.*, vol. 33, no. 10, pp. 4681–4687, Oct. 2019.

[11] Y. Zhu, Y. Zhang, and C. Yu, "Dynamic responses after rotor drops onto a new-type active eliminating protective clearance touchdown bearing," *J. Mech. Sci. Technol.*, vol. 34, no. 6, pp. 2277–2288, Jun. 2020.

[12] S. Yamada and H. Fujimoto, "Precise joint torque control method for two-inertia system with backlash using load-side encoder," *IEEJ J. Ind. Appl.*, vol. 8, no. 1, pp. 75–83, Jan. 2019.

[13] H. Jian, Z. Xinhua, Z. Zhaokai, W. Guan, W. Jingwei, and W. Xueqin, "The research of nonlinear factor characteristics and control method on large inertia electromechanical actuator servo mechanism," in *Proc. IEEE Transp. Electrific. Conf. Expo, Asia–Pacific (ITEC Asia-Pacific)*, Harbin, China, Aug. 2017, pp. 1–6.

[14] S. Yang and W. Jianli, "The influence and compensation of gear backlash on electric load system," in *Proc. 2nd Int. Conf. Frontiers Sensors Technol. (ICFST)*, Shenzhen, China, Apr. 2017, pp. 479–483.

[15] G.-W. Pan, W.-L. Chen, L.-P. Ding, and D.-L. Zhang, "Nonlinear dynamics modeling and backlash compensating of multi-stage gear transmission system," in *Proc. Int. Conf. Mater. Eng. Mech. Eng.*, Zhejiang, China, 2015, pp. 32–42.

[16] M. Dai, R. Qi, and Y. Li, "Switching control with time optimal sliding mode control strategy for electric load simulator with backlash," in *Proc. 22nd Int. Conf. Electr. Mach. Syst. (ICEMS)*, Harbin, China, Aug. 2019, pp. 1–6.

[17] Y. Zhang and P. D. Spanos, "Efficient response determination of a M-D-O-F gear model subject to combined periodic and stochastic excitations," *Int. J. Non-Linear Mech.*, vol. 120, Apr. 2020, Art. no. 103378.

[18] J. T. Kahnamouei and J. Yang, "Development and verification of a computationally efficient stochastically linearized planetary gear train model with ring elasticity," *Mechanism Mach. Theory*, vol. 155, Jan. 2021, Art. no. 104061.

[19] H. Xu, Y. Li, and L. Zhang, "A new control method for backlash error elimination of pneumatic control valve," *Processes*, vol. 9, no. 8, p. 1378, Aug. 2021.

[20] X. He, Z. Zhao, J. Su, Q. Yang, and D. Zhu, "Adaptive inverse control of a vibrating coupled vessel-riser system with input backlash," *IEEE Trans. Syst., Man, Cybern., Syst.*, vol. 51, no. 8, pp. 4706–4715, Aug. 2021.

[21] Z. Zhao, Z. Liu, W. He, K.-S. Hong, and H.-X. Li, "Boundary adaptive fault-tolerant control for a flexible Timoshenko arm with backlash-like hysteresis," *Automatica*, vol. 130, Aug. 2021, Art. no. 109690.

TONG FENG received the B.Sc. degree from the Harbin University of Science and Technology, China, in 2010, and the M.Sc. degree from Nottingham Trent University, U.K., in 2012. He is currently pursuing the Ph.D. degree with the Harbin Institute of Technology, China. His research interests include permanent magnet synchronous motor servo systems, its communication and control, and position sensor.

JIANAN SUN received the B.Sc. and M.Sc. degrees from the Harbin Institute of Technology, China, in 2018 and 2020, respectively. His research interests include mechanical structure and servo control.

JINJI QIU received the B.Sc. degree from the Harbin Institute of Technology, China, in 2019, where he is currently pursuing the M.Sc. degree. His research interests include circuit design and magneto-electric encoder.

SHUANGHUI HAO was born in Guizhou, China, in 1963. He received the B.Sc. degree from Tianjin University, in 1985, then began his research on special motor at Shanghai Electrical Apparatus Research Institute, China. After that, he received the M.Sc. and Ph.D. degrees from the Kyushu Institute of Technology, Japan, in 1997. He then went to YASKAWA Electric Corporation, Japan, and worked on AC servo motor. In 2003, he began to work with the Harbin Institute of Technology as a Professor. He is the author of more than 100 articles and has more than 60 patents. His research interests include magneto-electric encoder, AC servo systems, numerical control, and signal processing.